

# Dust Grain-Size Distributions From MRN to MEM

Geoffrey C. Clayton<sup>1</sup>, Michael J. Wolff<sup>2</sup>, Ulysses J. Sofia<sup>3</sup>, K. D. Gordon<sup>4</sup> and K. A. Misselt<sup>4</sup>

## ABSTRACT

Employing the Maximum Entropy Method algorithm, we fit interstellar extinction measurements which span the wavelength range 0.125-3  $\mu\text{m}$ . We present a uniform set of MEM model fits, all using the same grain materials, optical constants and abundance constraints. In addition, we are taking advantage of improved UV and IR data and better estimates of the gas-to-dust ratio. The model fits cover the entire range of extinction properties that have been seen in the Galaxy and the Magellanic Clouds. The grain models employed for this presentation are the simplistic homogeneous spheres models (i.e., Mathis, Rumpl, & Nordsieck 1977) with two (graphite, silicate) or three (graphite, silicate, amorphous carbon) components. Though such usage is only a first step, the results do provide interesting insight into the use of grain size as a diagnostic of dust environment. We find that the SMC Bar extinction curve cannot be fit using carbon grains alone. This is a challenge to the recent observational result indicating little silicon depletion in the SMC.

*Subject headings:* Extragalactic, extinction, dust, maximum entropy method, Magellanic Clouds

## 1. Introduction

It was suspected as long as 150 years ago that something was blocking the light of stars on its way to Earth, but it wasn't until the early twentieth century that the work of Barnard

---

<sup>1</sup>Department of Physics & Astronomy, Louisiana State University, Baton Rouge, LA 70803; Email: gclayton@fenway.phys.lsu.edu

<sup>2</sup>Space Science Institute, 3100 Marine Street, Ste A353, Boulder, CO 80303-1058; Email: wolff@colorado.edu

<sup>3</sup>Department of Astronomy, Whitman College, Walla Walla, WA 99362; E-mail: sofiauj@whitman.edu

<sup>4</sup>Steward Observatory, University of Arizona, Tucson, AZ 85721; E-mail: kgordon@as.arizona.edu, misselt@as.arizona.edu

and Trumpler confirmed the existence of obscuring clouds of interstellar dust (Whittet 1992 and references therein). Trumpler found that the wavelength dependence of interstellar extinction is proportional to  $\lambda^{-1}$  implying submicron size dust grains. Despite these early advances, we, in the early twenty-first century, are still struggling to understand the nature of cosmic dust. The chemical composition of the dust grains has been the most difficult problem to address since the available observational data do not provide strong constraints. Many solids have been suggested including ices, silicates, various carbon compounds, metals and complex organic molecules. Graphite has been a popular grain constituent since it was associated with the 2175 Å extinction bump (Stecher & Donn 1965). Two silicate features in the IR are widely observed providing one of the few firm identifications of a grain material (Woolf, & Ney 1969; Gillett, & Forrest 1973).

The best diagnostic for determining the sizes of interstellar dust grains is the wavelength dependence of extinction (Mathis 2000). A wealth of observational data now exists which characterizes extinction properties from the UV to the IR along sightlines in various dust grain environments. This combined with better constraints on the abundances of elements available for condensation into grains in the interstellar medium makes a study of the distribution of sizes of the dust grains into perhaps a slightly more tractable problem than it previously was. When data on the extinction were only available at visible wavelengths, the proposed size distribution was flat up to some cutoff size (Oort & van de Hulst 1946). The addition of data in the UV and IR wavelength regions in the last 40 years has revolutionized the study of the size distribution of dust grains, putting much more stringent constraints on the upper and lower size cutoffs and on the slope of the size dependence. The modern era of grain modeling was ushered in by Mathis, Rumpl, & Nordsieck (1977 [MRN]). Their grain model consisted of power-law size distributions of separate populations of bare spherical silicate and graphite grains. It is a testament to the groundbreaking nature of this work that today, twenty-five years later, it has not been fully superseded by later studies.

MRN-type analyses must make assumptions regarding a particular model of the size-dependence of the dust grains. One is now able to circumvent such issues through a solution of the inverse problem using the Maximum Entropy Method (MEM) (e.g., Kim, Martin, & Hendry 1994). The versatility of this technique allows one to easily include a range of grain models in the analysis: from the simple MRN-like approach to more realistic composite grains which can include the effects of porosity, solid inclusions (silicate, graphite, superparamagnetic etc.), and alignment. In this work, we present some preliminary efforts to extract MEM size distributions of dust grains in the Local Group using “basis sets” of grain cross-sections for several composite grain models, each of which satisfies cosmic abundance constraints.

## 2. History of Grain Size Distributions

Most studies of grain size over the last half century have assumed a size distribution which is either a power law or a power law with exponential decay (PED). In addition, most calculations have used Mie Theory assuming spherical grains. These power laws have been utilized for two reasons. First, they provide a good fit to the observed extinction wavelength dependence with as few as two populations of grains. Second, formation and destruction processes such as shattering and coagulation which modify grain sizes along many sightlines may naturally produce a power law size distribution (Biermann & Harwit 1980; Hayakawa & Hayakawa 1988; O’Donnell & Mathis 1997). This type of study began with Oort & van de Hulst (1946) who fit extinction at visible wavelengths assuming ice grains and a size distribution resembling a PED. Greenberg (1968) greatly expanded this work using spheres, cylinders and spheroids, combined with many different materials and grain orientations limited only by lack of computing power available at the time. Greenberg utilized the Oort & van de Hulst size distribution almost exclusively.

This brings us to MRN who found that a very good fit could be made to the UV and visible extinction using separate populations of bare silicate and graphite grains with a power law distribution of sizes where  $n(a) \propto a^{-3.5}$ . The graphite grains range in size from 0.005 to 1  $\mu\text{m}$  and the silicate grains from 0.025 to 0.25  $\mu\text{m}$ . Mathis & Wallenhorst (1981) expanded on MRN by showing that they could fit various high  $R_V^5$  sightlines with “peculiar” extinctions such as  $\sigma$  Sco,  $\rho$  Oph and  $\theta$  Ori by raising the lower size cutoff to 0.04  $\mu\text{m}$  and sometimes also raising the upper size cutoff. This suggested that small silicates are missing along these lines of sight. Greenberg & Chlewicki (1983) claimed that grains responsible for bump and FUV extinction are two independent populations and that MRN violates this condition. However, Cardelli, Clayton, & Mathis (1989 [CCM]) showed that the Greenberg & Chlewicki result is spurious due to having an  $R_V$  dependence in one ratio and not in the other.

The lack of accurate optical constants for silicates and graphite have cast doubts on the significance of the good fits to extinction data with MRN-type models. In the absence of laboratory data on graphite, MRN adjusted the optical constants to make the bump lie at 2175 Å. The situation improved with the work of Draine & Lee (1984) who synthesized dielectric functions for graphite and “astronomical” silicate on the assumptions that MRN is valid. The polycyclic aromatic hydrocarbon (PAH) absorption cross-section was established based on the interstellar 2175 Å bump profile (Li & Draine 2001). As data from the mid- and far-IR became available, it became evident that significant numbers of small grains and large

---

<sup>5</sup> $R_V$  is the ratio of total-to-selective extinction and is a crude measure of the average size of the dust grains along a particular line of sight.

molecules such as PAHs were needed to account for emission features and excess continuum emission from single-photon heating (Draine & Anderson 1985; Desert, Boulanger, & Puget 1990). The IRAS data imply a need to push the lower size cutoff of MRN down to  $\sim 0.0003 \mu\text{m}$ .

CCM suggested that all populations of grains are subject to the same processes in a systematic way across the whole size distribution. They found that there is an average Milky Way extinction relation,  $A(\lambda)/A(V)$ , over the wavelength range  $0.125 \mu\text{m}$  to  $3.5 \mu\text{m}$ , which is applicable to a wide range of interstellar dust environments, including lines of sight through diffuse dust, dark cloud dust, and star formation (CCM; Cardelli & Clayton 1991; Mathis & Cardelli 1992). The extinction relation is a function of one parameter, chosen to be  $R_V$ . The existence of this relation, valid over a large wavelength interval, suggests that the environmental processes which modify the grains are efficient and affect all grains. Mathis & Whiffen (1989) suggested that many grains are composite, perhaps like interplanetary grains with many individual grains of different materials including silicates and amorphous carbon stuck together in grains with significant amounts of vacuum. In their model, small bare graphite grains are still needed to explain the bump and PAHs for the IR.

MRN-type fits and the Draine & Lee optical constants have also been applied to sightlines in the the Magellanic Clouds. Pei (1992) constructed one characteristic curve for each of the Galaxy, LMC and SMC even though large variations are seen from sightline to sightline in the SMC and LMC let alone the Milky Way. He used data from Koornneef (1982, 1983), Rieke & Lebofsky (1985), Morgan & Nandy (1982), Nandy, Morgan, & Houziaux (1984) and Bouchet et al. (1985). This study did not use the best extinction curve data available even at that time. The wavelength dependence of UV extinction in the LMC and SMC are much better characterized now (Gordon & Clayton 1998; Misselt, Clayton, & Gordon 1999; Gordon et al. 2002). Pei (1992) uses the same exponent, and upper and lower cutoffs as MRN then varies the relative abundances of carbon and silicon in the three galaxies to get the best fit. He finds minor differences between the best fits and the measured curves, and suggests that changing the exponent and upper and lower cutoffs wouldn't improve on the fits presented. Pei finds it, "remarkable that all three parameters are roughly optimized for all three galaxies." The standard silicate/graphite model appears to account well for all of Pei's average curves with only the adjustment of the graphite to silicate ratio.

Aannestad (1995) expanded on MRN and extended fitting the extinction curve out to  $925 \text{ \AA}$  using Voyager data. He used both Mie calculations for spheres plus the discrete dipole approximation (DDA) for graphite disks. Large and small silicates and carbon grains, and PAHs were included along with organic refractory mantles (Jenniskens 1993). Aannestad suggests that the very small grains are made up of graphite, amorphous carbon, and diamond.

As with previous studies, the higher  $R_V$  extinction curves are fit by eliminating small grains. He also finds that 2:1 oblate graphite disks are better than spherical graphite for fitting the bump. Aannestad suggests that radiation pressure could be responsible for changing grain size distributions in addition to shattering and coagulation.

Aannestad’s study along with two that followed it (Mathis 1996; Li & Greenberg 1997) represent attempts to update MRN by addressing the complexities of fitting the UV to the far-IR extinction while staying within the constraint of the available abundances of various elements. The latter two studies use a PED for defining the size distribution. Mathis (1996) uses Mie theory but doesn’t attempt to include very small grains. Li & Greenberg (1997) employ finite cylinders for modeling the core-mantle grains. They state that their model uses less carbon than other models and so isn’t so constrained by the carbon abundance.

Dwek et al. (1997) fit dust models to IR emission from 3.5 to 1000  $\mu\text{m}$  using IRAS and COBE data. The IRAS data first showed cirrus emission with an excess at 12 and 25  $\mu\text{m}$  caused by fluctuations in small grains down to 3  $\text{\AA}$  in size. These may be the same as the PAHs that cause UIR bands. The Dwek et al. model uses bare silicate and graphite grains and PAHs. They make a fit to 14 parameters, 8 fixed and 6 varying, using Mie theory with the Draine & Lee constants. Once the IR emission was fit they calculated the predicted UV extinction for their derived size distribution.

In addition to the many MRN-like studies outlined above, two other methods have been suggested for deriving the dust grain size distribution by solving the inverse problem. Zubko, Krelowski, & Wegner (1996a, 1998) suggest regularization where once a grain model is assumed then a unique size distribution is derived. It is not restricted by any a priori relation such as a power law. However, like most of the other studies above, Zubko et al. use bare spherical grains (astronomical silicate, graphite, AC, SiC and water ice) and Mie theory to calculate the extinction efficiencies. Their best fit models are silicate/graphite/ice mixtures although, as they note, the 3.1  $\mu\text{m}$  ice feature is not seen in diffuse dust. Zubko et al. say the results are essentially different from the MRN power law. His method results in size distributions with more structure than a simple power law. They are qualitatively similar to the results of the MEM method described below. The regularization method has also been applied to the SMC extinction (Zubko 1999).

The other derivation of the size distribution is through the Maximum Entropy Method (MEM). Kim et al. (1994) use the MEM method with MRN-type bare spherical silicate, graphite and amorphous carbon particles for two cases with  $R_V = 3.1$  and 5.3. The main constraint applied is the wavelength dependence of interstellar extinction. A second constraint is the abundance of various elements. This is combined with an assumed gas-to-dust ratio,  $N_H/A_V$ . Their results are similar to MRN but the resulting size distribution has more

structure. The upper size cutoff in MRN was a subjective choice. MEM results show a smooth decrease starting at  $0.2 \mu\text{m}$ . The amounts of carbon and silicon used are similar to MRN. Solar abundances as defined by Grevesse & Anders (1989) were used to constrain their models. Kim & Martin (1996) expanded the MEM work to a wider range of  $R_V$  values. They fit  $R_V = 2.7$  to  $5.3$ , while trying to minimize amount of carbon used. They limited the mass to that used by  $R_V=3.1$ . They also found that fitting the extinction curve for  $\rho$  Oph needs more large particles in a bimodal distribution.

Recently, Weingartner & Draine (2001) expanded on MRN by establishing a multifunctional form of the grain sizes including two log-normal size distributions, PEDs and curvature terms. It involves 6 adjustable parameters for carbon grains and five for silicates. The fits are also constrained by  $R_V$  and the available carbon abundance. They fit extinction curves by varying the powers, the curvature parameters, the transition sizes, the upper cutoff parameters and the total volume per H atom in both the carbon and silicate grain distributions, respectively. They include sufficient numbers of small grains to account for observations of IR emission. They find carbon and silicate grain size distributions that can account for both the UV to IR extinction and the IR emission.

### 3. Elemental Abundances in the ISM

An important constraint on the composition of interstellar grains is the cosmic abundance of various elements. A proposed grain constituent cannot use more of any element than is available in the interstellar medium. So a set of reference abundances, that represent the typical ISM in a given galaxy, is needed. This set represents the total abundance of elements in the gas and dust. If these reference values are known, then a measurement of the gas phase abundances will reveal how much is missing, i.e., how much has condensed to form dust grains. In the last few years, new data have put much more stringent constraints on the reference abundances in the interstellar medium of the Galaxy (e.g., Spitzer & Fitzpatrick 1993; Cardelli et al. 1993, 1994; Sofia, Cardelli, & Savage 1994; Snow & Witt 1996). In particular, there was a move away from the use of solar abundances. This was motivated by the fact that solar abundances implied more oxygen than could be accounted for by the gas and solid phases of the ISM. As a result, it was suggested that all abundances may be about 60% of Solar. Other abundance sources such as B stars have been used instead. One impact of this has been the so-called “carbon crisis”, in which there may be less carbon available than is needed for various models of the interstellar extinction including MRN. In fact, Mathis (1996) shows this paucity of carbon would likely play a large role in constructing and validating grain models. Recently, however, it has become apparent that that the “crisis”

may be due to problems with the solar abundances. The measurements of the abundance of oxygen in the Sun have been dropping and now stand at about two thirds of its former value (Sofia & Meyer 2001). There is now no good argument for adopting a reference that is two-thirds the solar abundance (Sofia & Meyer 2001). Therefore, Solar abundances have been adopted as the standard for the the Galactic sightlines in this study. See Table 1.

In the Magellanic Clouds, the relative abundances between the elements are similar to those found in the local ISM (Russell & Dopita 1992; Welty et al. 1997; Venn 1999). However, the metallicities in the LMC and SMC are 0.3 and 0.6 – 0.7 dex lower, respectively, than in the local ISM in the Galaxy (Welty et al. 2001). Metallicity and the gas-to-dust ratio are correlated, so the amount of dust per hydrogen column is lower in the Magellanic Clouds.

The observed gas-phase abundances of various elements in the ISM should be just the reference abundance minus any depletion into dust grains. In the Galaxy, several depletion patterns have been associated with different environments (Savage & Sembach 1996; Welty et al. 2001). For example, the depletions range from -0.8 [Mg, Si/Zn] and -1.8 [Fe, Ni/Zn] to -0.2 [Mg, Si/Zn] and -0.5 [Fe, Ni/Zn] for cold dense clouds and the Galactic halo, respectively, with the warm diffuse ISM depletions lying in between. The relative gas-phase abundances in the Magellanic clouds resemble those in the Galactic halo implying that the depletion patterns in the ISM of those galaxies may be similar to those in the Galaxy despite the known differences in gas-to-dust ratio and metallicity (Welty et al. 2001). However, for at least three SMC sightlines, the depletion pattern shows one important difference. Silicon appears to be almost undepleted ( $< 0.2$  dex). Almost every grain model for the ISM from MRN to the present time includes silicates as an important constituent. In particular, grain models of the SMC have emphasized the importance of silicates since the role of carbon seems to be less important as measured by the strength of the 2175 Å feature (Pei 1992; Zubko 1999; Weingartner & Draine 2001). So, if silicon is indeed relatively undepleted in the SMC, the grain models will have to be reassessed (Welty et al. 2001).

#### 4. Extinction Curves

Low dispersion short and long wavelength IUE spectra, combined with BVJHK photometry were used to construct the extinction curves in this study. The spectra were downloaded from the MAST IUE archive. The archive spectra were reduced using NEWSIPS and then were recalibrated using the method developed by Massa & Fitzpatrick (2000). The short and long wavelength spectra for each star were co-added, binned to the instrumental resolution ( $\sim 5$  Å) and merged at the maximum wavelength of the short wavelength spectrum. Extinction curves were constructed using the standard pair method (e.g., Massa, Savage &

Fitzpatrick 1983). Uncertainties in the extinction curves contain terms that depend both on the broadband photometric uncertainties as well as those in the IUE fluxes, which are calculated directly in NEWSIPS. Our error analysis is described in detail in Gordon & Clayton (1998). The sample includes early-type supergiants which may be used with the same accuracy as main sequence stars in calculating extinction (Cardelli, Sembach, & Mathis 1992). Table 2 lists the sightlines being analyzed for this study.

The extinction curves have been fitted using the Fitzpatrick & Massa (1990, hereafter FM) parameterization. FM have developed an analytical representation of the shape of the extinction curves using a small number of parameters. This was done using linear combinations of a Drude bump profile,  $D(x; \gamma, x_o)$ , a linear background and a far-UV curvature function,  $F(x)$ , where  $x = \lambda^{-1}$ . There are 6 parameters determined in the fit: The strength, central wavelength, and width of the bump,  $c_3$ ,  $x_o$ , and  $\gamma$ , the slope and intercept of the linear background,  $c_1$  and  $c_2$ , and the strength of the far-UV curvature,  $c_4$ . The FM best fit parameters to the sightlines are given in Table 3.

Extinction data have been obtained from the literature for the LMC, SMC and some Galactic sightlines (Gordon & Clayton 1998; Misselt et al. 1999; Clayton, Gordon, & Wolff 2000). Various “average” curves have been calculated which generally represent extinction characteristics of groups of sightlines. In the SMC, only four suitable early-type stars have been observed that are significantly reddened and also had well matched comparison stars (Gordon & Clayton 1998). Three stars lie in the SMC Bar, and the line of sight for each of them passes through regions of recent star formation. The fourth star belongs to the SMC Wing and its line-of-sight passes through a much more quiescent region. In the LMC, the sample contains 12 stars in the 30 Dor region and 7 stars outside 30 Dor (Misselt et al. 1999). While the extinction properties of the 30 Dor and non-30 Dor samples as defined are both inhomogeneous, a group of stars with similar reddenings and bump strengths were found lying in or near the region occupied by the supergiant shell (LMC 2). The average extinction curves inside and outside LMC 2 show a very significant difference in 2175 Å bump strength, but the far-UV extinctions are very similar.

An “average” extinction curve for the Galaxy is included in Tables 2 and 3. It is representative of a typical diffuse interstellar sightline. It has been constructed by making an FM fit to a CCM curve with  $R_V=3.1$  (Misselt et al. 1999). Another average curve is included which represents dust characteristics along extremely long path length, low-density sightlines in the Galaxy from the sample of Sembach & Danks (1994, SD region) (Clayton et al. 2000). In addition, several individual sightlines are included in this study which are representative of the range of extinction characteristics seen in the Galaxy. They are listed in Table 2. These extinction curves have been constructed as described above (Valencic et



al. 2003). Extinction curves have been presented for these stars previously: HD 29647, HD 62542 (Cardelli & Savage 1988); HD 37022, HD 147889, HD 204827 (Fitzpatrick & Massa 1990); HD 147165 (Clayton & Hanson 1993); HD 210121 (Larson, Whittet, & Hough 1996); and the SD region (Clayton et al. 2000). These sightlines comprise values  $R_V$  from 2.1 to 5.5. The sample includes the “standard” CCM curve ( $R_V = 3.1$ ) as well as those with steep (HD 210121, SD Region, HD 204827) and flat (HD 37022, HD 147165, HD 147889) UV rises, normal and weak (HD 29647, HD 62542) bumps. These sightlines represent all the physical environments accessible to UV observations including dense clouds, star-forming regions and the diffuse ISM. In addition, we include average sightlines for the two extinction-curve types seen in each of the SMC and LMC.

## 5. Maximum Entropy Method

We employ a (slightly) modified version of the MEM extinction fitting algorithm developed by Kim et al. (1994, and references within). Instead of using the number of grains as a constraint, the algorithm employs the mass distribution:  $m(a) da =$  mass of dust grains per H atom in the size interval  $a$  to  $a+da$ . Thus, the traditional MRN-type model becomes  $m(a) \propto a^{-0.5}$ . We use a PED as the template function for each component. The data are examined at 34 wavelengths and the grain cross sections are computed over the range 0.0025-2.7  $\mu\text{m}$  with 50 logarithmically-spaced bins. The shape of the mass distribution is strongly constrained only for data over the region 0.04-1  $\mu\text{m}$ . Below 0.04  $\mu\text{m}$ , the Rayleigh scattering behavior constrains only total mass; above 1  $\mu\text{m}$ , the “gray” nature of the dust opacity also forces the MEM algorithm to simply adjust the total mass, using the shape of the template function to specify the size-dependence of the distribution.

The total mass of dust is constrained using both the gas-to-dust ratio and “cosmic” abundances (i.e., we try not to use more carbon or silicon than is available); see Table 1. As a first step, we consider only three-component models of homogeneous, spherical grains: modified “astronomical silicate” (Weingartner & Draine 2001), amorphous carbon (Zubko et al. 1996b), and graphite (Laor & Draine 1993).

We modeled all the individual and average sightlines for the Galaxy and the Magellanic Clouds listed in Table 2. The results are presented in Figures 1-3. For each sightline, two plots have been produced. The first shows the amount of extinction provided by each of the three materials, the total extinction of the model compared to the measured extinction curve. The fraction of the adopted abundance available for each material (Table 1) which is needed for the best model fit, is also listed. The second plot shows the resultant mass distribution for different sizes of grains of each material relative to the mass of hydrogen.

Figures 1 and 2 present the three-component models for a selection of Galactic sightlines including the “standard” curve ( $R_V = 3.1$ ). Figure 3 presents three-component models for the SMC and LMC curves described above.

## 6. Discussion

The MEM fits to all of the sightlines considered here show the same general behavior with the dust grain mass distributed across a wide range of sizes up to some upper size cutoff. As described above, the MEM model is not well constrained for very large and very small grains. One would naively think that as  $R_V$  gets larger and the UV extinction gets flatter that the relative amount of mass in small grains would go down and large grains would go up; for steeper curves, the opposite would happen. These effects are seen in Figures 1-3 but no simple correlation with  $R_V$  or far-UV steepness is seen. Similarly, sightlines with weak bumps use relatively less mass in the likely bump grains. One trend is that sightlines with higher than average gas-to-dust ratios lie below the average Galactic curve at all grain sizes. This is just due to the fact that the masses in the figures are normalized to the mass of hydrogen.

The fraction of the available silicon and carbon used in the MEM fits to the various sightlines covers a very wide range. Three general factors determine the fraction of silicon and carbon that any individual sightline will use. First, the higher the gas-to-dust ratio is, the more metals are available in the gas phase. Second, the higher the abundances of metals are, the more material is available. Finally, high values of  $R_V$  imply a greater than average mass fraction in larger grains. The extinction due to large grains is not as efficient per unit mass as smaller grains since the mass goes as  $a^3$  while the surface area goes as  $a^2$ . HD 37022 which has normal Galactic abundances and gas-to-dust ratio but the highest value of  $R_V$  in our sample, requires more than 100% of the available silicon and carbon. Similarly, the other high  $R_V$  sightlines, HD 147889, HD 147165 and HD 29647 all require large fractions of the available metals. The SMC Wing which has a low gas-to-dust ratio and low abundances also uses more than 100% of the available silicon and carbon. On the other hand, the SD region with a high gas-to-dust ratio, normal abundances and a low  $R_V$  uses less than half of the silicon and carbon. The LMC2 and the SMC Bar regions both have low abundances and high gas-to-dust ratios. Both use 50% or less of the available silicon and 60-80% of the carbon. The SMC Bar uses a larger fraction of both elements because of its higher normalized extinction, requiring more dust grains. The relationship between elemental fraction used and the gas-to-dust ratio is illustrated in Figure 4.

All extinction models rely heavily on silicates, yet recent observations suggest that

silicon is relatively undepleted in the SMC Bar (Welty et al. 2001). It should be noted that the sightlines investigated by Welty et al. do not have extinction curves due to their small reddenings. However, MEM model fits to the average SMC Bar extinction indicate that the curve cannot be fit with carbon grains alone. Since there is almost no bump in the SMC Bar extinction that may also imply the presence of fewer graphite grains. Carbon grains are responsible for most of the visible extinction and silicon grains for most of the UV extinction. So, in general, both species of grains are needed along any sightline to get a good fit to the extinction curve. At least, the MEM fit for the SMC Bar requires a smaller fraction of silicon and carbon than almost any other sightline modeled.

A quick look at the figures shows that the HD 210121 and SMC Bar sightlines are the most unusual in their grain size distributions. Both differ strongly from the CCM curve. These two sightlines also have the steepest far-UV extinction. The model fits show a deficit of large silicate and amorphous carbon grains for both sightlines. The HD 210121 sightline which, unlike the SMC Bar, has a significant bump, shows a slightly larger size cutoff for graphite grains. The next steepest sightlines, in the LMC and in the SD region in the Galaxy do not show much difference from the average curve once the gas-to-dust ratio differences are taken into account. The importance of small grains in the steep UV rise for several sightlines (including HD 204827) is also quite evident. Larson et al. (2000) also did MEM modeling for HD 210121 with similar results. The largest  $R_V$  sightline, toward HD 37022, also shows large deviations from the average Galactic curve. The MEM fit to the HD 37022 sightline shows a large deficit of small graphite and silicate grains. Kim et al. (1994) found that extinction with  $R_V=5.3$  requires a similar dust mass to extinction with  $R_V=3.1$ . There is a great reduction in the number of grains with sizes less than  $0.1 \mu\text{m}$  and some increase in larger particles for the model with the larger value of  $R_V$ . Among the fits to other large  $R_V$  sightlines, HD 147165 shows trends similar to the HD 37022 fit while the fit to HD 147889 is not significantly different from the average Galactic fit. The mass distributions, found in this study, show significant departures from power-law (and even PED) behavior. This is an important distinction to make in light of the work by Pei (1992), which extends MRN to the same environments by changing only the end points of the grain size range.

As an interesting exercise, we constructed a composite model along the lines of Mathis (1998). However, given our interest in increasing the cross section per unit volume while also minimizing the amounts of Si and C used, we chose to explore the use of pyroxene and oxides. In other words, by freeing up some of the [Fe,Mg] normally used in olivine-like astronomical silicate, one is able to form oxides without consuming any additional cosmic Fe or Mg (as compared to olivine). Briefly, our composite grain component consists of (by volume) 28.5% pyroxene ( $[Fe_{0.6}Mg_{0.4}]SiO_3$ ), 16.5% amorphous carbon, 5% oxide ( $[Fe_{0.4}Mg_{0.6}]O$ ), and 50% vacuum. The elemental budget for this component is  $[C/H] = 1.05\text{e-}4$  and  $[Si/H] = 2.9\text{e-}5$ .

Defining a “molecule” of this material to have 1 Si atom, one derives a molecular weight of 213 and density of  $1.45 \text{ g/cm}^3$ . The dust mass densities used in this study are  $\rho_{sil} = 3.3 \text{ g cm}^{-3}$ ,  $\rho_{gra} = 2.3 \text{ g cm}^{-3}$  and  $\rho_{amc} = 1.8 \text{ g cm}^{-3}$ . We included small silicates and small carbon (graphite) grains in our composite model, in addition to the composite grain component itself.

Following the lead of Mathis (1998), we computed the optical properties using a geometric mean of two effective medium mixing rules: Bruggeman and an extension by Ossenkopf (1991). The dielectric functions for the individual components were taken from the following sources: amorphous carbon - Be form of Zubko et al. (1996b); oxide - Henning et al. (1995), and pyroxene - Dorschner et al. (1995). Unfortunately, the latter two are limited to wavelengths above  $0.22 \mu\text{m}$  (we discarded the  $0.2 \mu\text{m}$  point). For the purpose of this exercise, we assumed that the UV behavior of the materials will be similar to that of astronomical silicates (i.e., the Fe component is dominant in this regime). So, we extended the dielectric function to the  $0.08\text{--}0.2 \mu\text{m}$  region by scaling the imaginary component ( $k$ ) of astronomical silicates to match smoothly with that of each material at  $0.22 \mu\text{m}$ . We then computed the real component ( $n$ ) using a subtractive Kramers-Kronig (SKK) algorithm, implementation kindly supplied by Kelly Snook (Snook 1999; see also Warren 1984). The fixed-point value of  $n$  needed for the SKK calculations is adopted from the visible measurements of each material at a wavelength of  $0.5 \mu\text{m}$ . The model fits are shown in Figure 5. This result is intriguing as it indicates that the composite grains may require a smaller fraction of the available silicon and carbon.

Weingartner & Draine (2001) note that Kim et al. (1994) make more efficient use of the grain volume by using MEM to construct more complicated size distributions. They find this “fine-tuning unappealing.” However, their own models have trouble staying within the standard abundance/depletion limits. Weingartner & Draine suggest that it is more likely that the abundance constraints are too stringent and the real Galactic abundances are higher than solar. As can be seen in Figures 1 and 3 of this paper, the MEM model fits sometimes require 100% or more of the available silicon and carbon assuming the “new” old solar abundances. Weingartner & Draine fit the Galactic average extinction curve as well as the average LMC, LMC2 and SMC Bar sightlines. A comparison of their results with ours shows significant differences, in particular, in the upper size cutoffs of silicate and carbon grains. For example, Weingartner & Draine also fit the HD 210121 sightline. Their two-component fit has upper size cutoffs of  $\sim 0.3 \mu\text{m}$  for the silicates and  $\sim 1 \mu\text{m}$  for carbonaceous grains. In our three-component fit, we find the opposite,  $\sim 0.3 \mu\text{m}$  for amorphous carbon and  $\sim 1 \mu\text{m}$  for silicate grains. We also include graphite with an upper cutoff of  $\sim 0.3 \mu\text{m}$ . Dwek et al. (1997) used IR emission at mid-IR wavelengths to constrain the size distribution and then predicted the UV extinction. They find a size distribution for silicates not too different

from MRN and include two power laws for graphite. Their predicted UV extinction curve is steeper in the UV than the  $R_V=3.1$  extinction curve. The cirrus, modeled by Dwek et al. (1997), is located at high latitude so may have extinction more like that seen toward HD 210121. The differences among these studies reinforce the fact that while the model results are useful, they are not unique. Li & Greenberg (1998) fit the extinction curve of HD 210121 using both an MRN power-law with silicates and graphite, and a core-mantle model.

Most previous papers that calculate the size distributions assume just one “average” extinction curve to fit (i.e., Mathis 1996). In this paper, we present a uniform set of MEM model fits, all using the same grain materials, optical constants and abundance constraints. In addition, we are taking advantage of improved UV and IR data and better estimates of the gas-to-dust ratio. The model fits cover the entire range of extinction properties that have been seen in the Galaxy and the Magellanic Clouds.

Clearly, more work needs to be done: The derived mass distributions will need to be tested in other observational regimes, such as thermal IR and linear polarization. More sophisticated cross sections need to be included, both in terms of grain topology and composition. The next step will include composite grains, as well as both aligned and randomly-oriented spheroids. In addition, more extensive Galactic studies need to be undertaken. Specifically, attempts to tie sightline characteristics such as depletion patterns, molecular abundances, etc. to specific extinction features (i.e., steep UV rise, weak bump).

We would like to thank Kelly Snook for her help with this project. This work was supported by NASA ATP grant NAG5-9203.

## REFERENCES

- Aannestad, P.A. 1992, *ApJ*, 443, 653  
Biermann, P. & Harwit, M. 1980, *ApJ*, 241, L105  
Bohlin, R. C., Savage, B. D., & Drake, J. F. 1978, *ApJ*, 224, 132  
Bouchet, P., Lequeux, J., Maurice, E., Prevot, L., & Prevot- Burnichon, M.L. 1985, *A&A*, 149, 330  
Cardelli, J.A., & Clayton, G.C. 1991, *AJ*, 101, 1021  
Cardelli, J. A., Clayton, G. C., & Mathis, J. S. 1989, *ApJ*, 345, 245  
Cardelli J.A., Mathis, J.S., Ebbets, D.C., & Savage, B.D. 1993, *ApJ*, 402, L17  
Cardelli, J. A., & Savage, B.D. 1988, *ApJ*, 325, 864

- Cardelli, J.A., Sembach, K.R., & Mathis, J.S. 1992, *AJ*, 104, 1916
- Cardelli J.A., Sofia, U.J., Savage, B.D., Keenan, F.P., & Dufton, P.L. 1994, *ApJ*, 420, L29
- Clayton, G.C., Gordon, K.D., and Wolff, M.J. 2000, *ApJS*, 129, 147
- Clayton, G.C., & Hanson. M.M. 1993, *A.J.*, 105,1880
- Clayton, G. C., Wolff, M. J., Allen, R. G., & Lupie, O. L. 1995, *ApJ*, 445, 947
- Clayton, G. C., Wolff, M. J., Gordon, K.D., & Misselt, K.A. 2000, *ASP Conf. Ser.*, 196, 41
- Desert, F.-X., Boulanger, F., & Puget, J.L. 1990, *A&A*, 237, 215
- Dorschner J., Begemann B., Henning Th., Jaeger, C., & Mutschke, H. 1995, *A&A*, 300, 503
- Draine, B.T., & Anderson, N. 1985, *ApJ*, 292, 494
- Draine, B.T., & Lee, H.M. 1984, *ApJ*, 285, 89
- Dwek, E. et al. 1997, *ApJ*, 475, 565
- Fitzpatrick, E. L. 1985, *ApJ*, 299, 219
- Fitzpatrick, E. L. & Massa, D. 1990, *ApJS*, 72, 163
- Gillett, F.C., & Forrest, W.J. 1973, *ApJ*, 179, 483
- Gordon, K. D. & Clayton, G.C. 1998, *ApJ*, 500, 816
- Gordon, K. D., Clayton, G.C., Misselt, K.A., Wolff, M.J., & Landolt, A.U. 2002, *ApJ*, Submitted
- Greenberg, J.M. 1968, in *Nebulae and Interstellar Matter*, ed. B.M. Middlehurst and L.H. Aller (Chicago: University of Chicago Press), p. 221
- Greenberg, J.M., & Chlewicki, G. 1983, *ApJ*, 272, 563
- Grevesse,N., & Anders, E. 1989, in *Cosmic Abundances of Matter*, *AIP Conf. Proc.*, 183, 1
- Gunderson, K. A., Clayton, G. C., & Green, J. 1998, *PASP*, 110, 60
- Hayakawa, H., & Hayakawa, S. 1988, *PASJ*, 40, 341
- Henning Th., Begemann B., Mutschke H., & Dorschner J. ,1995, *A&AS*, 112, 143
- Jenniskens, P. 1993, *A&A*, 274, 653
- Kim, S.-H. & Martin, P. G. 1995, *ApJ*, 442, 172
- Kim, S.-H. & Martin, P. G. 1996, *ApJ*, 462, 296
- Kim, S.-H., Martin, P. G., & Hendry, P.D. 1994, *ApJ*, 422, 164
- Koornneef, J. 1982, *A&A*, 107, 247
- Koornneef, J. 1983, *A&A*, 128, 84

- Laor, A. & Draine, B. T. 1993, ApJ, 402, 441
- Larson, K.A., Whittet, D.C.B., & Hough, J.H. 1996, ApJ, 472, 755
- Larson, K.A., Wolff, M.J., Roberge, W.G., Whittet, D.C.B., & He, L. 2000, ApJ, 532, 1021
- Li, A., & Draine, B.T. 2001, ApJ, 554, 778
- Li, A., & Greenberg, J.M. 1997, A&A, 323, 566
- Li, A., & Greenberg, J.M. 1997, A&A, 339, 591
- Martin, N., Maurice, E., & Lequeux, J. 1985, A&A, 215, 219
- Massa, D., & Fitzpatrick, E. L. 2000, ApJS, 126, 517
- Massa, D., Savage, B. D., & Fitzpatrick, E. L. 1983, ApJ, 266, 662
- Mathis, J. S. 1996, ApJ, 472, 643
- Mathis, J. S. 1998, ApJ, 497, 824
- Mathis, J. S. 2000, JGR, 105, 10269
- Mathis, J. S., & Cardelli 1992, ApJ, 398, 610
- Mathis, J. S., Rumpl, W. & Nordsieck, K.H. 1977, ApJ, 217, 425
- Mathis, J. S., & Wallenhorst, S.G. 1981, ApJ, 244, 483
- Mathis, J. S., & Whiffen, G. 1989, ApJ, 341, 808
- Misselt, K. A., Clayton, G. C., & Gordon, K. A. 1999, ApJ, 512, 128
- Morgan, D.H., & Nandy, K. 1982, MNRAS, 199, 979
- Nandy, K., Morgan, D.H., & Houziaux, L. 1984, MNRAS, 211, 895
- O'Donnell, J.E., & Mathis, J.S 1997, ApJ, 479, 806
- Oort, J.H., & van de Hulst, H.C. 1946, BAN, 10, 187
- Ossenkopf, V. 1991, A&A, 251, 210
- Pei, Y. C. 1992, ApJ, 395, 130
- Rieke, G.H., & Lebofsky, M.J. 1985, ApJ, 288, 618
- Rouleau & Martin 1991, ApJ, 377, 526
- Russell, S. C. & Dopita, M. A. 1992, ApJ, 384, 508
- Savage, B.D., Drake, J.F., Buditch, W., & Bohlin, R.C. 1977, ApJ, 215, 788
- Savage, B.D., & Sembach, K.R. 1996, ARA&A, 34, 279
- Sembach, K.R., & Danks, A.C. 1994, A&A, 289, 539

- Snook, K. J., 1999, Ph.D Thesis, Stanford University, Stanford, California
- Snow, T.P., & Witt, A.N. 1996, ApJ, 468, L65
- Sofia, U.J., Cardelli, J.A. & Savage, B.D. 1994, ApJ, 430, 650
- Sofia, U.J., & Meyer, D.M. 2001, ApJ, 554, L221
- Spitzer, L., & Fitzpatrick, E.L. 1993, ApJ, 409, 299
- Stecher, T.P., & Donn, B. 1965, ApJ, 142, 1681
- Valencic, L. et al. 2002, in preparation
- Venn, K.A. 1999, ApJ, 518, 405
- Warren, S., 1984, Appl. Opt., 23, 1206
- Weingartner, J.C., & Draine, B.T. 2001, ApJ, 548, 296
- Welty, D. E., Lauroesch, J.T., Blades, J.C., Hobbs, L.M., & York, D.G. 1997, ApJ, 489, 672
- Welty, D. E., Lauroesch, J.T., Blades, J.C., Hobbs, L.M., & York, D.G. 2001, ApJ, 554, L75
- Whittet, D.C.B. 1992, Dust in the Galactic Environment, (IOP: Bristol)
- Whittet, D.C.B., Gerakines, P.A., Hough, J.H., & Shenoy, S.S. 2001, ApJ, 547, 872
- Whittet, D.C.B., Martin, P.G., Fitzpatrick, E.L., & Massa, D. 1993, ApJ, 408, 573
- Woolf, N.J., & Ney, E.P. 1969, ApJ, 155, L181
- Zubko, V.G. 1999, ApJ, 513, L29
- Zubko, V.G., Krelowski, J., & Wegner, W. 1996a, MNRAS, 283, 577
- Zubko, V.G., Krelowski, J., & Wegner, W. 1998, MNRAS, 294, 548
- Zubko, V.G., Mennella, V., Colangeli, L., & Bussoletti, E. 1996b, MNRAS, 282, 1321



Table 1. Adopted Abundances.

	“Cosmic”		In Dust		References
	Si/H	C/H	Si/H	C/H	
Galactic	4.0e-5	3.2e-4	3.8e-5	1.8e-4	1
Galactic (Halo)	4.0e-5	3.2e-4	2.0e-5	1.8e-4	1
SMC	1.1e-5	5.4e-5	1.1e-5	5.4e-5	2,3
LMC	6.5e-5	1.1e-4	6.5e-5	1.1e-4	2,4

Note. — 1. Sofia & Meyer 2001, 2. Russell & Dopita 1992,  
3. Welty et al. 1997, 4. Welty et al. 1999

Table 2. Observational Characteristics of the Modeled Sightlines.

Sightline	$R_V$	$E_{B-V}$	$N_H/E_{B-V}$	References <sup>a</sup>
SMC Bar	2.7	0.18	3.6e+22 <sup>b</sup>	1,2,18
SMC Wing	2.1	0.24	1.5e+21 <sup>b</sup>	1,3,18
LMC	3.4	0.25	1.1e+22	4,5,18
LMC 2	2.8	0.19	1.9e+22	4,5,18
Average Galactic	3.1	...	5.8e+21	6,7
HD 29647	3.6	1.00	5.8e+21	6,12
HD 37022	5.5	0.34	5.8e+21	6,7
HD 62542	3.2	0.33	5.8e+21	6,11,13
HD 147165	3.8	0.40	5.9e+21 <sup>b</sup>	7,14,15
HD 147889	4.2	1.09	5.8e+21	7
HD 204827	2.6	1.10	5.8e+21	6,8
HD 210121	2.1	0.38	5.8e+21	9,10
SD Region <sup>c</sup>	2.7	0.24	1.2e+22 <sup>b</sup>	16,17

<sup>a</sup> (1) Gordon & Clayton 1998, (2) Martin et al. 1989, (3) Fitzpatrick 1985, (4) Gunderson et al. 1998, (5) Misselt et al. 1999, (6) Bohlin et al. 1978, (7) CCM, (8) Clayton et al. 1995, (9) Larson et al. 1996, (10) Larson et al. 2000, (11) Cardelli & Savage 1988, (12) Whittet et al. 2001, (13) Whittet et al. 1993, (14) Clayton & Hanson 1993, (15) Savage et al. 1977, (16) Clayton et al. 2000, (17) Sembach & Danks 1994, (18) Gordon et al. 2002

<sup>b</sup>  $N_{HI}/E_{B-V}$

<sup>c</sup> Average of 7 sightlines (Clayton et al. 2000)

Table 3. FM Parameters

Sightline	$c_1$	$c_2$	$c_3$	$c_4$	$x_o$	$\gamma$	Ref.
SMC Bar	$-4.47 \pm 0.19$	$2.35 \pm 0.18$	$0.08 \pm 0.01$	$-0.22 \pm 0.004$	–	–	1
SMC Wing	$-1.00 \pm 0.15$	$1.17 \pm 0.12$	$3.49 \pm 0.19$	$0.17 \pm 0.04$	$4.69 \pm 0.0001$	$1.17 \pm 0.05$	1
LMC	$-1.28 \pm 0.34$	$1.11 \pm 0.10$	$2.73 \pm 0.37$	$0.64 \pm 0.06$	$4.596 \pm 0.017$	$0.91 \pm 0.05$	2
LMC 2	$-2.16 \pm 0.36$	$1.31 \pm 0.08$	$1.92 \pm 0.23$	$0.42 \pm 0.08$	$4.626 \pm 0.010$	$1.05 \pm 0.07$	2
Milky Way	$0.12 \pm 0.11$	$0.63 \pm 0.04$	$3.26 \pm 0.11$	$0.41 \pm 0.02$	$4.596 \pm 0.002$	$0.96 \pm 0.01$	2
HD 29647	$-0.02 \pm 0.20$	$0.82 \pm 0.02$	$3.06 \pm 0.26$	$0.61 \pm 0.25$	$4.64 \pm 0.03$	$1.45 \pm 0.003$	4
HD 37022	$2.06 \pm 0.35$	$0.004 \pm 0.003$	$2.14 \pm 0.06$	$0.53 \pm 0.04$	$4.56 \pm 0.002$	$1.04 \pm 0.02$	4
HD 62542	$-1.31 \pm 0.06$	$1.31 \pm 0.09$	$2.64 \pm 0.10$	$1.36 \pm 0.12$	$4.61 \pm 0.01$	$1.37 \pm 0.02$	4
HD 147165	$1.07 \pm 0.20$	$0.31 \pm 0.02$	$4.03 \pm 0.12$	$0.04 \pm 0.003$	$4.59 \pm 0.002$	$1.09 \pm 0.02$	4
HD 147889	$1.89 \pm 0.20$	$0.09 \pm 0.018$	$4.77 \pm 0.05$	$0.92 \pm 0.04$	$4.62 \pm 0.01$	$1.08 \pm 0.01$	4
HD 204827	$-0.74 \pm 0.08$	$1.10 \pm 0.01$	$3.11 \pm 0.11$	$0.86 \pm 0.16$	$4.60 \pm 0.01$	$1.16 \pm 0.02$	4
HD 210121	$-3.15 \pm 0.09$	$1.96 \pm 0.15$	$2.94 \pm 0.15$	$1.05 \pm 0.11$	$4.57 \pm 0.01$	$1.11 \pm 0.02$	4
SD Region	$-1.83 \pm 0.14$	$1.19 \pm 0.20$	$1.52 \pm 0.27$	$0.58 \pm 0.10$	$4.60 \pm 0.02$	$0.93 \pm 0.02$	3

Note. — (1) Gordon et al. 2002, (2) Misselt et al. 1999, (3) Clayton et al. 2000, (4) Valencic et al. 2002

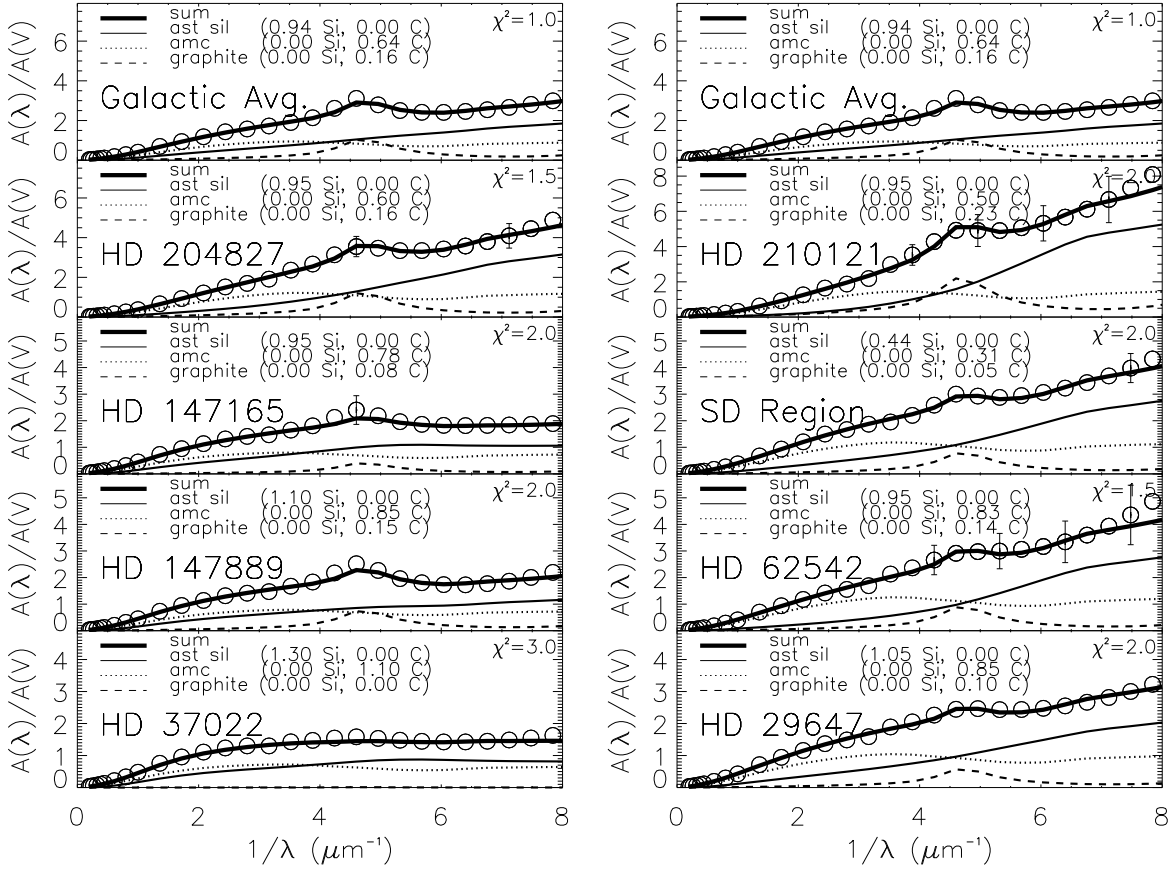


Fig. 1.— Three-component extinction models for Galactic sightlines. Each panel shows the model fit to the extinction curve, including the contribution of each component. The fraction of the “cosmic” Si and C (amorphous carbon and graphite) utilized is listed in the figure legend (See Table 1 for abundances).

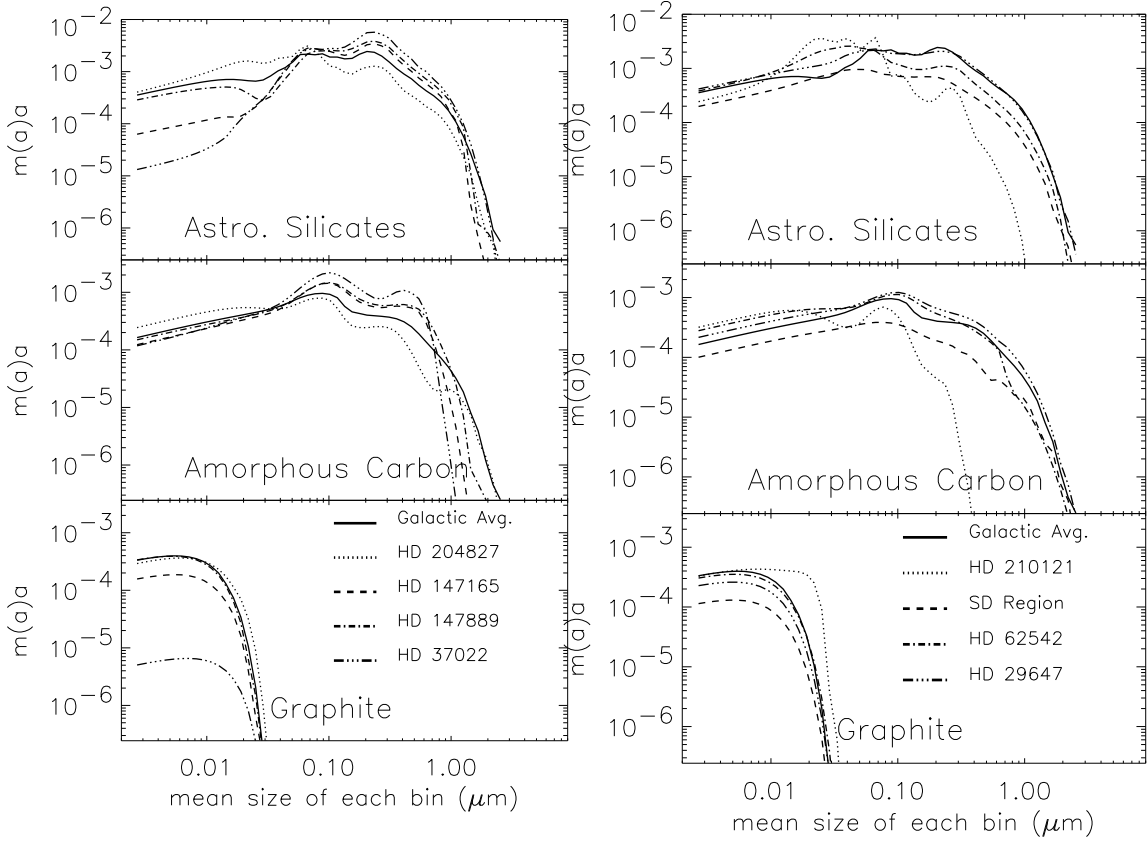


Fig. 2.— Three-component extinction models for Galactic sightlines. Each panel contains the resultant mass distributions relative to the mass of hydrogen. For the three-component model, amorphous carbon replaces graphite as primary source of carbonaceous continuum extinction. In order to minimize the graphite requirement in the three-component model, we adopt a new template function; size bins are included only through  $0.04 \mu\text{m}$ .

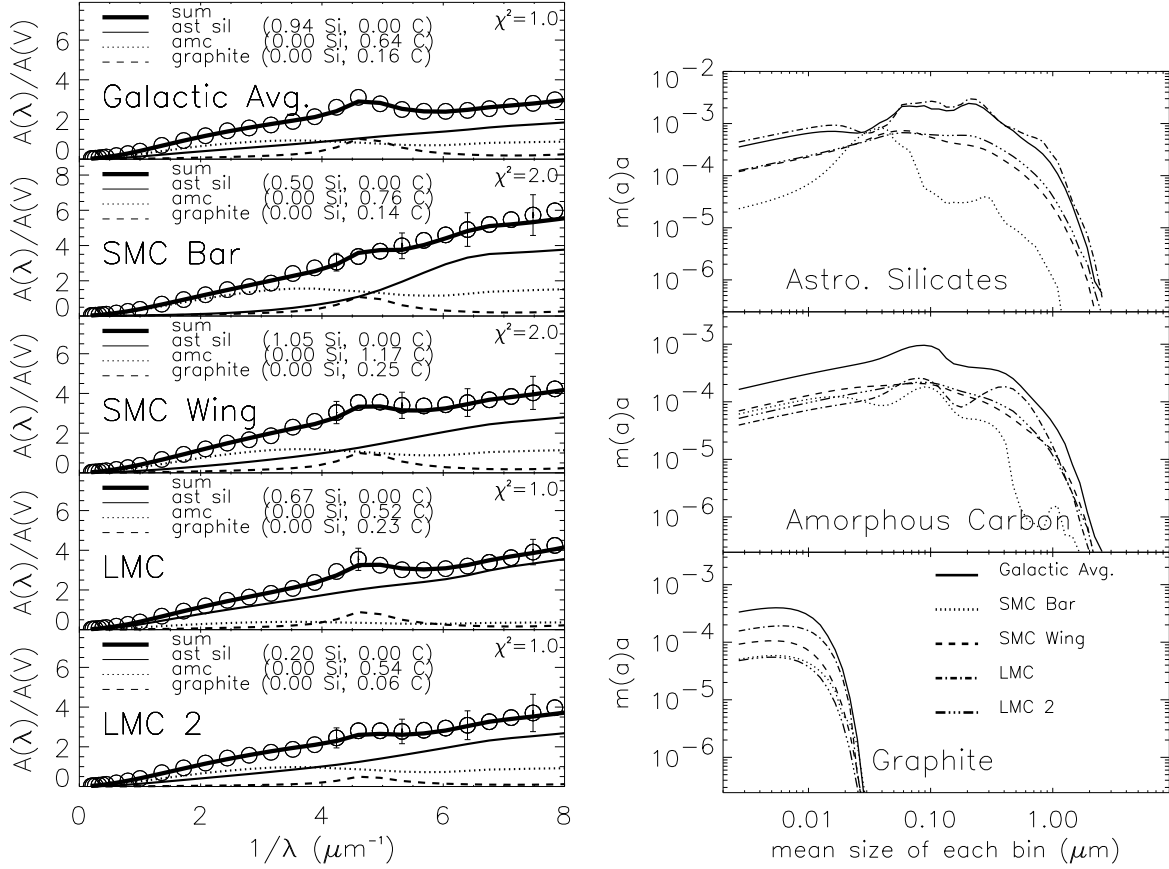


Fig. 3.— Three-component extinction modes for Magellanic Cloud sightlines. The left-hand panel shows the model fits to the extinction curves, including the contribution of each component. The right-hand panel contains the resultant mass distributions relative to the mass of hydrogen. Plotted in the same way as Figures 1 and 2.

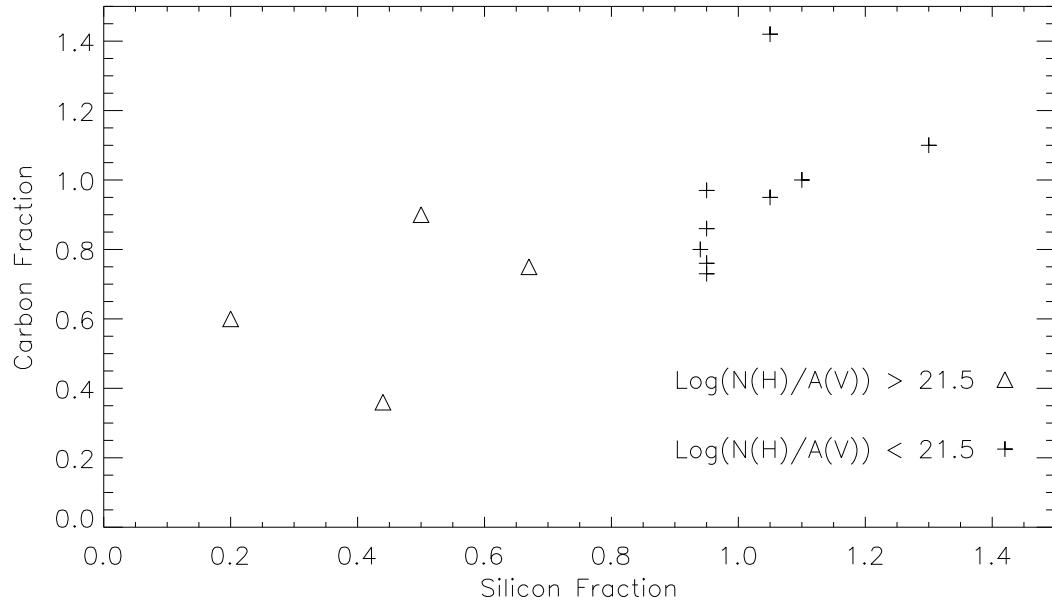


Fig. 4.— Fraction of available silicon used plotted against fraction of available carbon (amorphous carbon + graphite) used for the sightlines in our sample. The sample has been divided into those with large and small values of the gas-to-dust ratio.

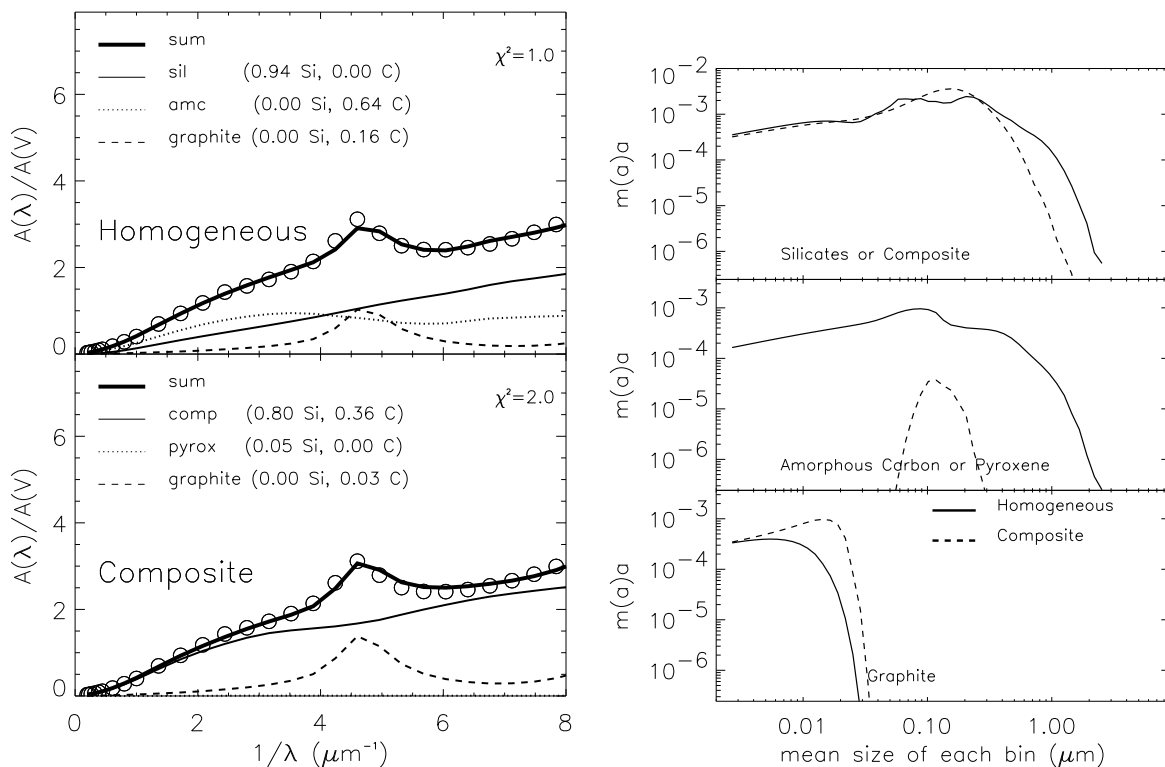


Fig. 5.— Composite model including pyroxene and oxides for the average Galactic extinction compared to the 3-component fit used in Figures 1 and 2. The left-hand panel shows the model fits to the extinction curves, including the contribution of each component. The right-hand panel contains the resultant mass distributions relative to the mass of hydrogen. Plotted in the same way as Figures 1 and 2.